STAR Note # 422
22 May, 2000

Simulation Study of Characteristics of the EndCap Electromagnetic Calorimeter for the STAR detector

N.D. Gagunashvili, O.V. Rogachevski, M.V. Tokarev, Yu.A. Panebratsev

Laboratory of High Energies,
Joint Institute for Nuclear Research,
141980, Dubna, Moscow region, Russia

L.C. Bland, S.E. Vigdor

Indiana University Cyclotron Facility,
Bloomington, IN47408, USA

P. Nevski

Brookhaven National Laboratory,
P.O.Box 5000, Upton New York 11973-5000, USA

H. Spinka

Argonne National Laboratory,
Argonne, IL 60439, USA

Abstract

The endcap electromagnetic calorimeter (EEMC) increases the physics capability of the STAR detector to study high-p_T and polarization phenomena in pp and pA collisions. In this paper we present a Monte Carlo study of the EEMC performance proposed by the Indiana University group. A geometrical description of the EEMC is implemented in the GSTAR framework. The basic characteristics of the EEMC such as energy and position resolution, and linearity of responses are studied using full GEANT simulation.

1 Introduction

The Relativistic Heavy Ion Collider (RHIC) gives unique possibilities [1] to study fundamental physics phenomena, such as the nature of proton spin and a possible phase transition of nuclear matter.

Important contributions in understanding of spin structure of the proton were obtained from a series of polarized deep inelastic scattering experiments performed at SLAC [3, 4, 5], CERN [6] and DESY [7]. Numerous analyses of experimental data on the spin-dependent structure function g_1 in the framework of perturbative QCD have shown that additional information on the spin-dependent gluon distribution ΔG is necessary to unambiguously determine the contributions of the sea quarks of different flavors to the proton spin [8, 9]. The study of asymmetry of direct photon, jet, dijet and γ+jet production in $\vec{p}+\vec{p}$ collisions is more relevant for the direct measurement of $\Delta G(x, Q^2)$ [10, 11, 12, 13]. Electroweak production of intermediate bosons $(W^{\pm}, Z^0)$ and measurements of a single asymmetry A_L^W are preferred to separate quark and antiquark spin- and flavor-dependent distributions [14]. The spin program with polarized protons colliding at RHIC is part of the scientific program of STAR [13, 15].

High-p_T direct photons, dileptons and jets are good probes of dense matter formed in ultra-relativistic heavy-ion collisions that are the central focus of RHIC. Hard quark-gluon or gluon-gluon collision processes are responsible for hadron and lepton production over a high transverse momentum range. Therefore the study of hadron spectra in pp and their modifications in pA and AA collisions is very important in searching for a phase transition of nuclear matter to a quark-gluon plasma and the limits to physics analysis based on perturbative QCD.

Thus the entire RHIC spin and heavy-ion programs are complementary to each other. Both require the installation of the electromagnetic calorimeter inside the STAR magnet.

The barrel electromagnetic calorimeter (BEMC) is a finely segmented lead-scintillator sampling calorimeter [2]. The acceptance of the BEMC covers a range $|\eta| < 1$ and 2π in azimuth. The effective acceptance of the BEMC for jets is $|\eta| < 0.3$. The proposed endcap electromagnetic calorimeter (EEMC) [16] expands the acceptance of the STAR detector from the pseudorapidity range $|\eta| < 1$ to $-1.0 \leq \eta < 2.0$. It is expected that the EEMC significantly increases the experimental statistics for the direct γ and jet production. The EEMC provides high spatial and energy resolution detection capabilities in regions far from mid-rapidity and access to the phase space region characterized by the greatest sensitivity to ΔG.

A crucial issue in determining the direct photon yield is the experimental distinction between directly produced photons and photon pairs coming from electromagnetic decays of neutral mesons, especially π^0 and η^0. It was shown in [16] that the use of an isolation cut is not sufficient to identify direct photons cleanly. Therefore the EEMC has the shower-maximum detector (SMD) which allows additional discrimination between single photons and photon pairs on the basis of the measured transverse profile of the electromagnetic shower.

In this paper a Monte Carlo study of the basic characteristics of the EEMC is performed. The detailed geometrical description of the EEMC design proposed by the Indiana University group in the AgSTAR framework is given in Sec.2. Characteristics of the EEMC and SMD are described in Sec.3. Conclusions are summarized in Sec.4.

2 Geometrical description of the EEMC

For this simulation study the geometrical description for the new design of the endcap EMC is done in the AgSTAR framework [17]. The construction of the EEMC is illustrated in Fig.1, where the cross-section of the endcap wheel is shown.

The endcap EMC covered $1.07 \leq \eta \leq 2.$ in pseudo-rapidity. The front plate is 3/8" aluminum and the back plate 7/8" stainless steel. According to the proposal [16] the calorimeter volume is divided into twelve 30° modules. The segmentation is made by defining a constant 5 intervals in ϕ and 12 intervals in η. So the calorimeter is divided in 720 elementary volumes – towers. Each of the towers spans approximately 0.1 unit in azimuthal angle ϕ and from 0.057 to 0.102 units in η. The gradual change in η segmentation is made with definition a constant ratio in pseudo-rapidity between the small and large angle edge of each tower $\eta_{high}/\eta_{low} = 1.0536$.

Each tower consists of twenty three layers of lead and twenty four layers of plastic scintillator, arranged in an alternating pattern. A cross section of layers is shown in detail in Fig.2. The scintillator tiles are each 4 mm in thickness, with the exception of the first two – preshower layers, where the thickness is increased to 5 mm. Each scintillator tile is followed by a 1.6 mm plastic sheet for fiber routing and 1 mm of clearance. The absorbing layers comprise 4.68 mm thick Pb sheets clad with two 0.5 mm stainless steel plates. In the layer before the back plate there is no absorber Pb/SS plate.

The shower maximum detector (SMD) is located after the fifth Pb/SS layer in the modules. The geometrical structure of the SMD is shown in Fig.3. For simplicity we take here a similar depth layout of the SMD layer for all calorimeter modules. It is made from plastic scintillator strips of triangular cross section (1 cm base by 0.5 cm apex height), organized into orthogonal u and v planes. The two planes will have a $\pm 45°$ strip orientation with respect to the radial line bisecting each sector. There are 300 strips in each plane. The depth for the u-plane in the SMD is taken to be 7.5 mm and 17 mm for the v-plane. The u-plane scintillator strips are mounted on a 1.5 mm thick aluminum plate and the v-plane on a 1 mm plate. The rest of the SMD volume is filled out with plastic spacers.

For simulating the electromagnetic showers in the endcap EMC/SMD the thresholds have been chosen to be 1 MeV for electrons/positrons and 80 keV for γ quanta in Pb and scintillator materials.

3 Characteristics of EEMC and SMD

In this Section the basic physical characteristics of the EEMC such as energy response, deposited energy distribution, linearity of calorimeter response, energy and position resolutions are studied using a Monte Carlo GEANT simulation. The geometrical structure of the EEMC described above in AgSTAR is used. MC simulation is used to test the geometrical file for the EEMC.

3.1 Energy response

The electromagnetic calorimeters are necessary for energy measurements on photons, leptons and jets. Simulation results of 2000 gammas with $\eta = 1.5$, $\phi = 1.57$ and energy 30 GeV are shown in Figs.4(a-d).

The deposited energy distribution for a single photon is illustrated in Fig.4(a). It can be seen that the sampling fraction is approximately 1.4 $GeV/30\ GeV = 0.047$.

The electromagnetic showers are initiated by photons of various energies. The position of the maximum of the shower and depth of a shower energy deposition are determined by critical energy ϵ for lead. The electromagnetic shower profile of the EEMC for γ's with energy 30 GeV is shown in Fig.4(b). The total radiation length of the EEMC is about (21-27)X_0.

The shower-maximum detector provides the fine spatial resolution required to locate and identify photons and electrons and crucial photon/neutral-meson and electron/hadron particle discrimination.

Figs.4(c) and 4(d) show the simulated average u- and v- responses of the SMD for 30 GeV direct photons as a function of strip.

3.2 Linearity of calorimeter response

The absolute energy deposited in each tower must be determined sufficiently well over the entire dynamic range to satisfy minimum requirements for all measurement parameters. The linearity of energy calorimeter response or energy calibration characterizes quantitatively a possibility to accurately reconstruct an incident photon energy.

To study the dependence between deposited energy in the EEMC and incident energy of gammas a special set of events was prepared. It consists of 1000 γ's for each energy 2.5, 5, 10, 20, 40, 80 and 160 GeV. The direction of γ's was taken to be $\eta = 1.5$ and $\phi = 1.57$. A Gaussian fit of the deposited energy distribution for each energy gives the mean values μ, $\Delta\mu$, σ and $\Delta\sigma$.

Fig. 5(a) shows the mean value μ with errors $\Delta\mu$ as a function of photon energy. The fit of this dependence with the law $E_{dep} = aE_\gamma$ gives $a \simeq 0.0479$. The reconstructed energy of gammas can be defined by the formula $E_{rec} = E_{dep}/0.0479$.

Fig. 5(b) demonstrates the ratio E_{rec}/E_γ or the relative linearity of EEMC response as a function of incident photon energy. The relative linearity was found to be better than 2.% at $E_\gamma > 5\ GeV$.

The deposited energy distribution in the SMD as a function of photon energy is shown in Fig. 6. The distribution is described by $E_{dep} = d \cdot E_\gamma^{0.71}$. The value of the parameter d was found to be 0.016 and 0.015 for u- and v-plane, respectively.

3.3 Energy resolution

The energy resolution is one of the important characteristics of the EEMC. Assuming the energy resolution of the EEMC follows the law $\sigma(E)/E = b/\sqrt{E} \oplus c$, the parameters b and c were found to be 15.6% and 0.8%, respectively. The results of the MC simulation are presented in Fig.7(a). The resolution $\sigma(E)/E$ as a function of $E^{-1/2}$ is shown in Fig.7(b).

The simulated results of the energy resolution of the endcap SMD are shown in Figs.8(a) and 8(b). One can see that a linear dependence of $\sigma(E)/E$ as a function of $E^{-1/2}$ at $E < 20\ GeV$ takes place.

3.4 Position resolution

The endcap SMD should provide a high spatial resolution for better γ/π^0 discrimination. The u and v position of the photon intersection in u and v planes are determined by the classical formula for the mode

$$u = u_0 + \frac{h}{2} \cdot \frac{(E_2 - E_1)}{(E_2 - E_1) + (E_2 - E_3)}.$$

Here u_0 is a low edge of a strip with maximal response (modal strip) in cm; h is a strip width (1cm); E_1 is the response of the strip preceding the modal strip; E_2 is the response of the modal strip; E_3 is the response of the strip following the modal strip.

The distribution of the u-position defined above for gammas with energy 2.5 GeV and $\eta = 1.5$, $\phi = 1.57$ is shown in Fig.9. A Gaussian fit of this distribution gives the u-position resolution σ_u. The same method was used to obtain the v-position resolution σ_v.

The dependence of the u- and v-position resolutions on photon energy E_γ is shown in Fig.10. The results are obtained by using the mode reconstruction method. One can see that u- and v-position resolutions improve with increasing photon energy and reach 0.14 and 0.19 mm at $E_\gamma = 80\ GeV$, respectively.

4 Conclusions

The geometrical description for the new design of the endcap EMC proposed by the Indiana University group in the AgSTAR framework was done. A full GEANT simulation study of the basic characteristics of the EEMC such as deposited energy distributions, linearity of calorimeter response, and energy and position resolution was performed. The relative linearity response for photons over the energy range 5. – 160 GeV was found to be better than 2.%. The energy resolution of the EEMC for γ's $\sigma/E = 15.6\%/\sqrt{E} \oplus 0.8\%$ is close to the value achieved with BEMC. The new design of the endcap SMD provides the u- and v-position resolutions for 2.5 GeV photons $\sigma_u = 0.78\ mm$ and $\sigma_v = 0.9\ mm$, respectively. The resolution improves as photon energy increases and reaches $\sigma_u = 0.14$ and $\sigma_v = 0.19$ at $E_\gamma = 80\ GeV$.

Acknowledgments

The authors would like to thank V.Dunin for useful discussion and remarks of the present work.

References

[1] STAR Collaboration, M.E. Beddo et al., "The Conceptual Design Report for the Solenoidal Tracker At RHIC", LBL, PUB-5347; J. Harris et al., (STAR Collaboration) Nucl. Phys. **A566** (1994) 277.

[2] STAR Collaboration, M.E. Beddo et al., "The Conceptual Design Report for the Electromagnetic Calorimeter for Solenoidal Tracker At RHIC", LBL, PUB-5380.

[3] SLAC E142 Collaboration, P.L. Anthony et al., Phys. Rev. Lett. **71** (1993) 95; Phys. Rev. **D54** (1996) 6620.

[4] SLAC E143 Collaboration, K. Abe et al., Phys. Rev. Lett. **74** (1995) 346; Phys. Rev. Lett. **75** (1995) 25; Phys. Lett. **B364** (1995) 61;

[5] SLAC E154 Collaboration, K. Abe et al., Phys. Rev. Lett. **79** (1997) 26; Phys. Lett. **B405** (1997) 180.

[6] SMC Collaboration, D. Adams et al., Phys. Rev. **D56** (1997) 5330; D. Adeva et al., Phys. Lett. **B302** (1993) 533; D. Adams et al., Phys. Lett. **B357** (1995) 248; D. Adams et al., Phys. Lett. **B396** (1997) 338. D. Adeva et al., Phys. Lett. **B412** (1997) 414.

[7] HERMES Collaboration, K. Ackerstaff et al., Phys. Lett. **B404** (1997) 383.

[8] T. Germann, W.J. Stirling, Phys. Rev. **D53** (1996) 6100.

[9] E. Leader, A. Sidorov, D.B. Stamenov, Int. J. Mod. Phys. **13** (1998) 5573.

[10] M.V. Tokarev, G.P.Škoro, Nuovo Cimento **A111** (1998) 353.

[11] G.P.Škoro, M. Zupan, M.V. Tokarev, Nuovo Cimento **A112** (1999) 2227.

[12] R. G. Badalian, S. Heppelmann, Phys. Rev. **D57** (1998) 4367.

[13] S.E. Vigdor, In: Proceedings 13 International Symposium on High Energy Spin Physics, September 8-12, 1998, Protvino Russia, eds. N.E. Tyurin et al., World Scientific Publishing Co. Pte. Ltd. p.151.

[14] C. Borrely, J. Soffer, F. M. Renard, P.Taxil, Phys. Rep. **177** (1989) 319.

[15] G. Bunce et al., Particle World **3** (1992) 1; Proceedings of RIKEN BNL Research Center Workshop "RHIC Spin Physics", April 27-29, 1998, Report BNL-65615. Org. G. Bunce et al. (1998).

[16] L.C. Bland et al., "The Conceptual Design Report for the Endcap Electromagnetic Calorimeter for STAR", STAR Note# 401, 15 June, 1999.

[17] P. Nevski, "Advanced Geometry Interface for GSTAR", 28 April, 1996.

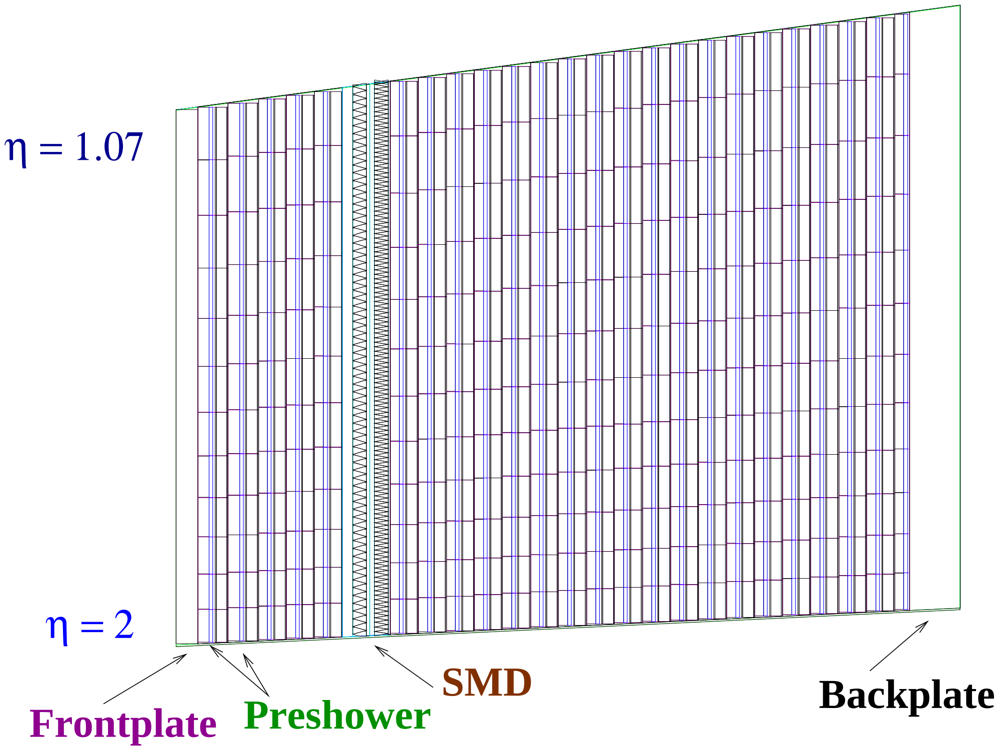

Figure 1. The schematic view of a cut through the EEMC.

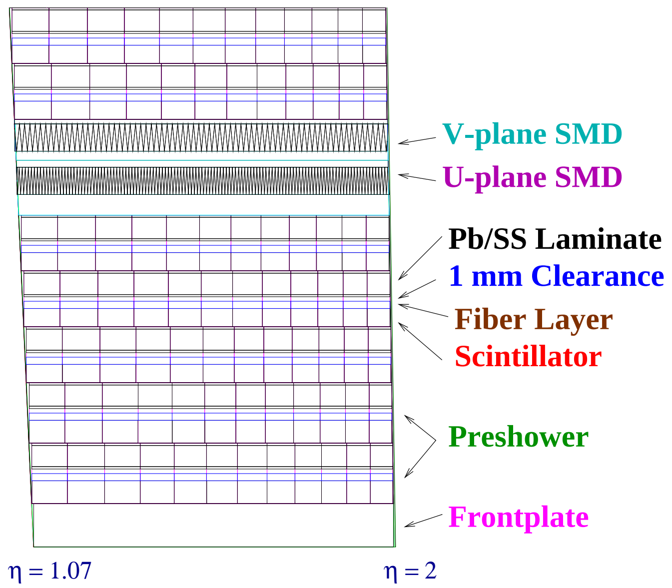

Figure 2. The schematic view of front part of a cut through the EEMC.

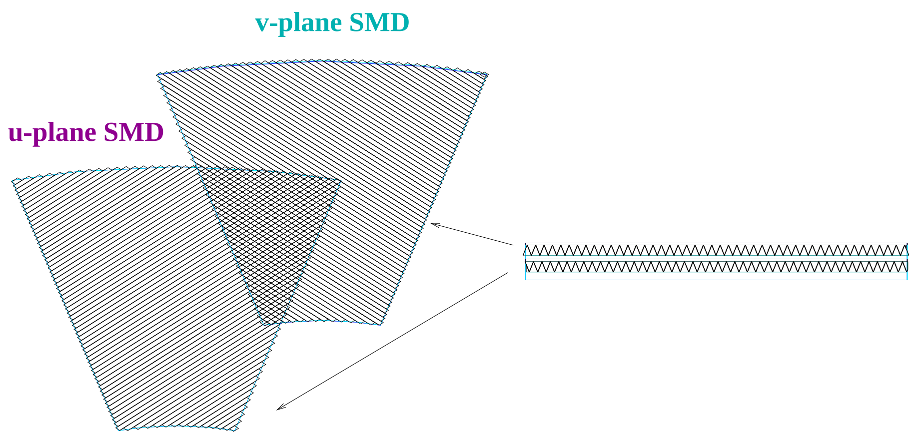

Figure 3. The schematic view of one 30^0 sector of the EEMC SMD.

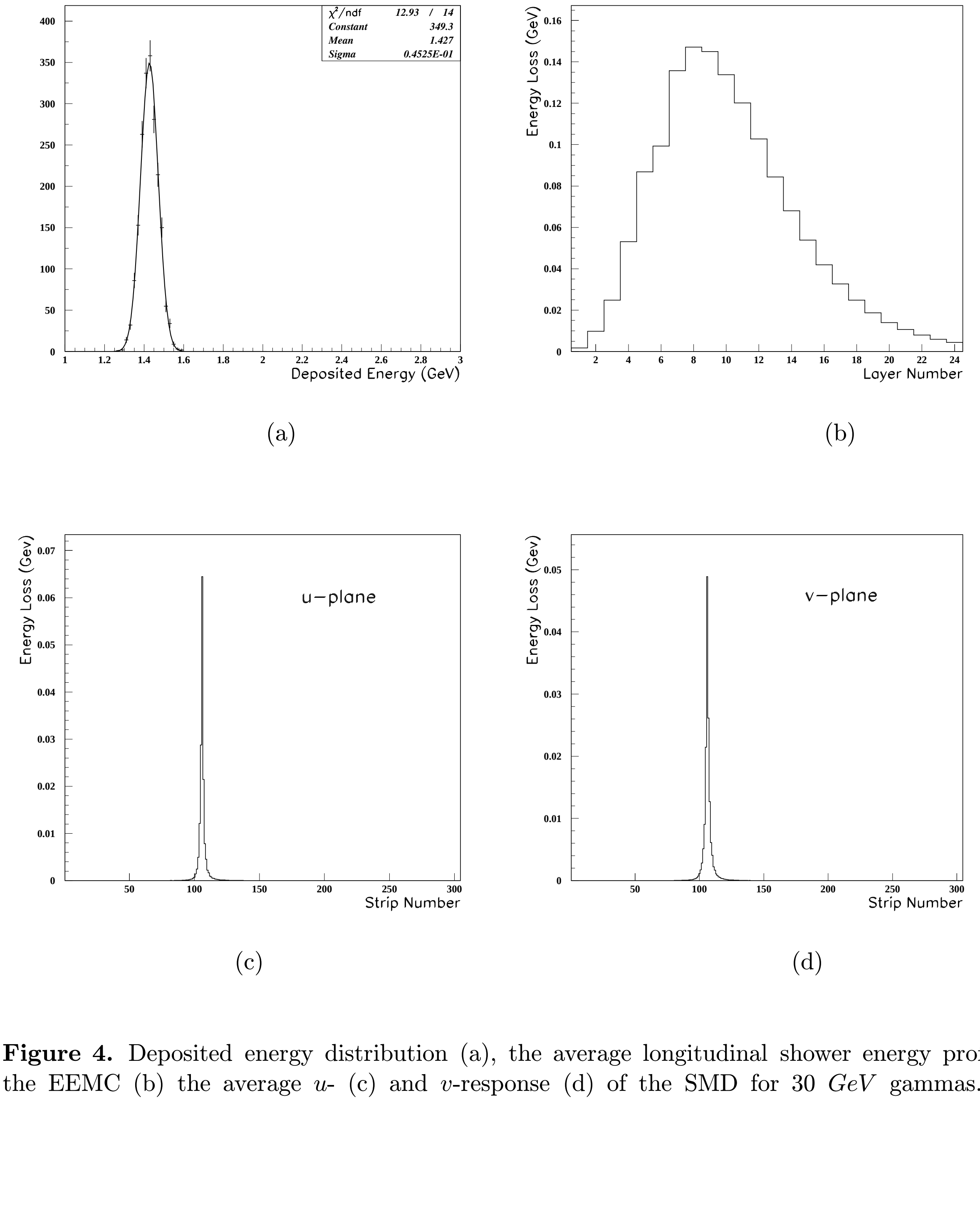

Figure 4. Deposited energy distribution (a), the average longitudinal shower energy profile of the EEMC (b) the average u- (c) and v-response (d) of the SMD for 30 GeV gammas.

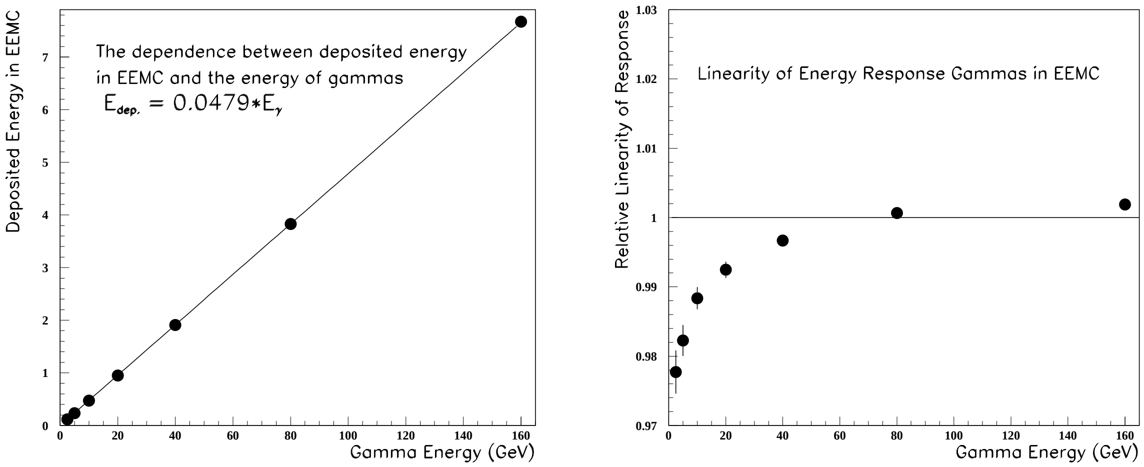

(a) (b)

Figure 5. (a) Dependence between deposited energy of the EEMC and incident photon energy. (b) Relative linearity of energy response of the EEMC for gammas.

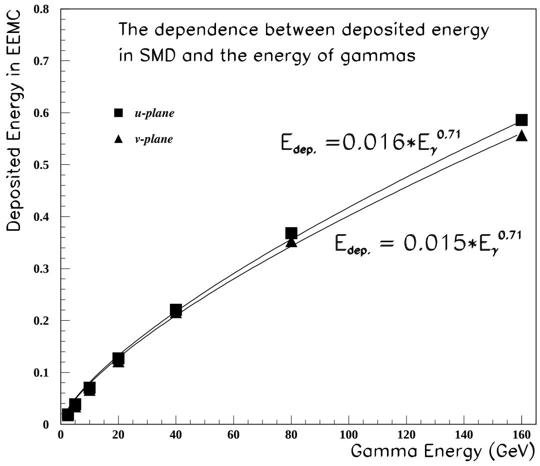

Figure 6. Dependence between deposited energy of the SMD and incident photon energy.

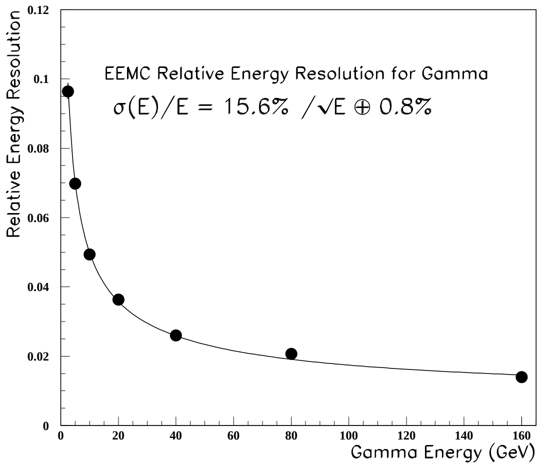

(a)

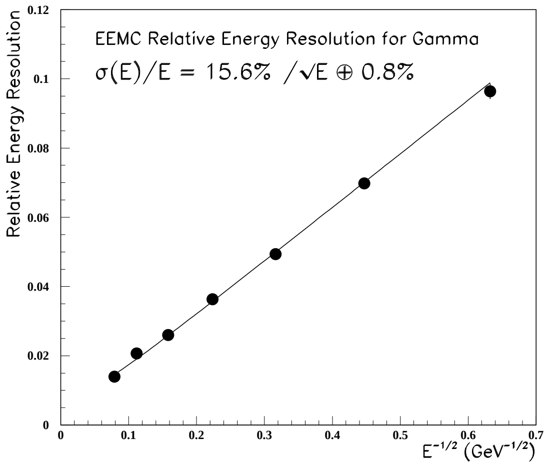

(b)

Figure 7. EEMC relative energy resolution for gammas $\sigma(E)/E$ as a function of E (a) and of $E^{-1/2}$ (b).

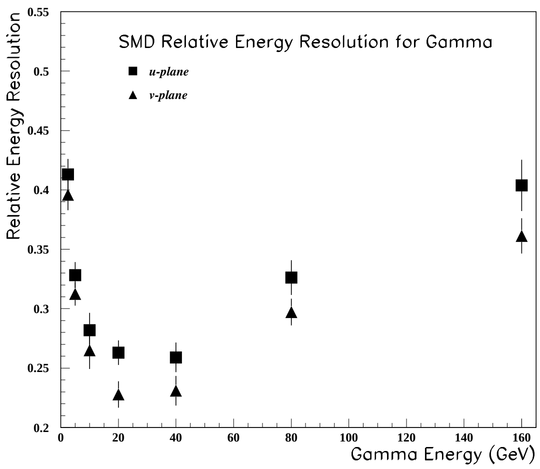

(a)

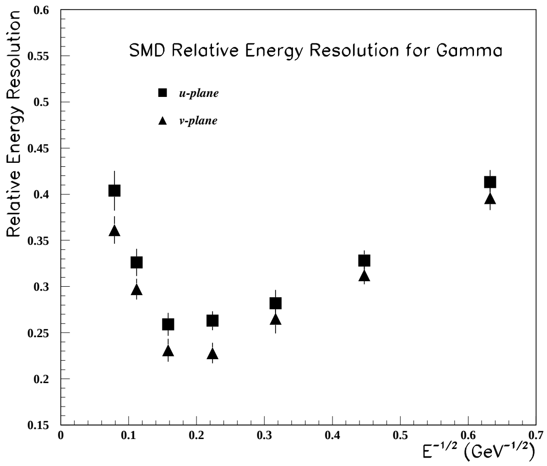

(b)

Figure 8. SMD relative energy resolution for gammas as a function $\sigma(E)/E$ as a function of E (a) and of $E^{-1/2}$ (b).

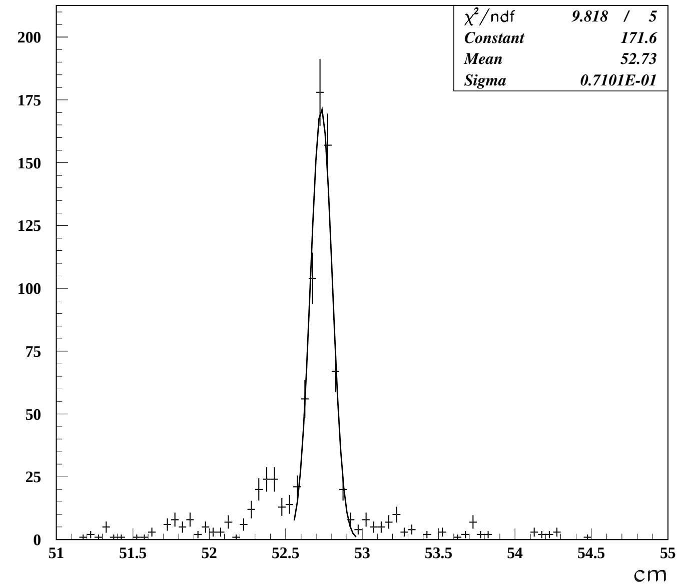

Figure 9. Distribution of u-position for 2.5 GeV gammas reconstructed by the mode method.

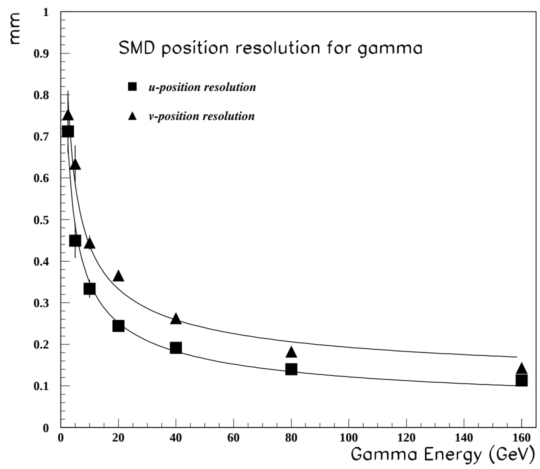

(a)

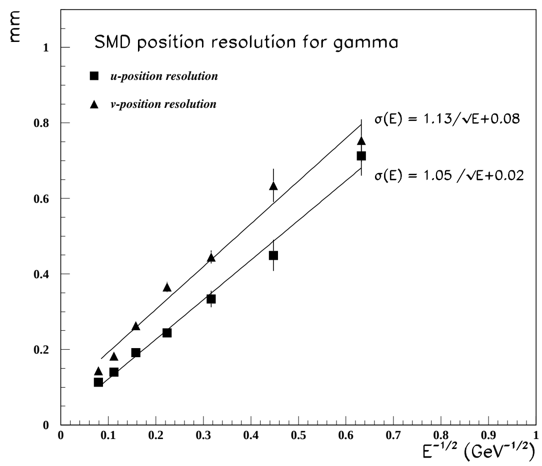

(b)

Figure 10. Energy dependence of SMD u- and v-position resolutions for gammas. Results are obtained by the mode reconstruction method.